

NANO EXPRESS

Open Access



# A Novel Magnetoelastic Nanobiosensor for Highly Sensitive Detection of Atrazine

Shengbo Sang<sup>1†</sup>, Xing Guo<sup>1†</sup>, Rong Liu<sup>1</sup>, Jingzhe Wang<sup>1</sup>, Jinyu Guo<sup>1</sup>, Yixia Zhang<sup>1,2</sup>, Zhongyun Yuan<sup>1</sup> and Wendong Zhang<sup>1\*</sup>

## Abstract

Here, we firstly report a wireless magnetoelastic (ME) nanobiosensor, based on ME materials and gold nanoparticles (AuNPs), for highly sensitive detection of atrazine employing the competitive immunoassay. In response to a time-varying magnetic field, the ME material longitudinally vibrates at its resonance frequency which can be affected by its mass loading. The layer of AuNPs coating on the ME material contributes to its biocompatibility, stability, and sensitivity. The atrazine antibody was oriented immobilized on the AuNPs-coated ME material surface through protein A, improving the nanobiosensor's performance. Atomic force microscope (AFM) analysis proved that the immobilization of atrazine antibody was successful. Furthermore, to enhance the sensitivity, atrazine–albumin conjugate (Atr–BSA) was induced to compete with atrazine for binding with atrazine antibody, amplifying the signal response. The resonance frequency shift is inversely and linearly proportional to the logarithm of atrazine concentrations ranging from 1 ng/mL to 100 µg/mL, with the sensitivity of 3.43 Hz/µg mL<sup>-1</sup> and the detection limit of 1 ng/mL, which is significantly lower than the standard established by US Environmental Protection Agency (EPA). The experimental results indicated that the ME nanobiosensor displayed strong specificity and stability toward atrazine. This study provides a new convenient method for rapid, selective, and highly sensitive detection of atrazine, which has implications for its applications in water quality monitoring and other environmental detection fields.

**Keywords:** ME nanobiosensor, ME materials, AuNPs, Atrazine detection

## Introduction

With the rapid development of industry and agriculture, more and more environmental contaminants were released into the ecological environment [1], which caused widespread concern about the relevant researches [2, 3]. In recent years, herbicides have been used in increasing amounts to improve quality and yield in agriculture fields, but many herbicides can remain active in water and soils for years causing serious environmental pollution [4]. Herbicide pollution has attracted considerable attention due to its ecological contamination in water or in agriculture products [5]. Among herbicides, atrazine (2-chloro-4-ethylamino-6-isopropylamino-1, 3, 5-triazine) is the most extensively

used for broad-leaf plants and grassy weeds control around the world [6].

Although atrazine has certain inhibitory effect on some perennial weeds, as the environmental contaminant, it is highly toxic [7] and may cause health risks for humans and other animal species [8]. Long-term high concentrations of atrazine intake can impair animal or human health, such as cancer, birth defects, and damage to the heart and liver [9, 10]. The USA, the European Union, and Japan have all included atrazine in the list of endocrine-disrupting chemicals [11]. In the USA, the Environmental Protection Agency (EPA) allows the permissible limit 3 µg/L (Lifetime Health Advisory Level) of atrazine in drinking water [12]. Thus, it is necessary to accurately quantify atrazine at low concentrations.

Many conventional analytical techniques have been developed for atrazine detection, including LC coupled to mass spectrometry (LC–MS) [13], high-performance liquid chromatography (HPLC) [14], and gas chromatography

\* Correspondence: [mnsrctyut@163.com](mailto:mnsrctyut@163.com)

<sup>†</sup>Shengbo Sang and Xing Guo contributed equally to this work.

<sup>1</sup>MicroNano System Research Center, Key Lab of Advanced Transducers and Intelligent Control System of the Ministry of Education & College of Information Engineering, Taiyuan University of Technology, Jinzhong 030600, China

Full list of author information is available at the end of the article

coupled also with mass spectrometry (GC–MS) [15], but these methods also have some limitations, such as high-cost, need of large instruments, poor selectivity, and time-consuming [16].

As a wireless mass-sensitive platform, the magnetoelectric (ME) sensor made from ME material has been widely developed for various applications due to their critical advantages of low cost, high sensitivity, smaller size, and ease of use [17, 18]. Currently, ME sensors are usually made of amorphous ferromagnetic alloys materials, such as Metglas 2826 MB ( $\text{Fe}_{40}\text{Ni}_{38}\text{Mo}_4\text{B}_{18}$ ) [19]. Under the externally applied alternating and static magnetic fields, the ME material longitudinally vibrates at its resonance frequency [20], generating a magnetic flux density that can be wirelessly detected by a pickup coil without any direct physical connections [21]. According to Eq. (1) [22], the fundamental resonance frequency  $f_0$  depends on the material length  $L$ , density  $\rho$ , elastic modulus  $E$ , and Poisson's ratio  $\nu$ .

$$f_0 = \frac{1}{2L} \sqrt{\frac{E}{\rho(1-\nu^2)}} \quad (1)$$

A small additional mass load  $\Delta m$  deposited on the ME material surface of mass  $M$  ( $\Delta m \ll M$ ) causes a shift in the resonance frequency ( $\Delta f$ ), which is given by Eq. (2) [23].

$$\frac{\Delta f}{\Delta m} = -\frac{f_0}{2M} \quad (2)$$

Based on above unique properties of the ME material, the resonance frequency of the ME material decreases with an increase of the extra mass load. Thus, through their functionalization with a sensing film, the ME materials have been developed for physical, chemical, and biological analysis, such as the detection of stress/pressure [24], temperature/humidity [25], carbon dioxide [26], endotoxin [27], *Salmonella typhimurium/Bacillus anthracis* spores [28], and *Escherichia coli* O157:H7 [29]. To our knowledge, however, no application of the ME material has been applied on the atrazine detection.

In this research, utilizing its excellent properties and advantages, we firstly proposed a wireless ME nanobiosensor employing the ME material as the substrate and gold nanoparticles (AuNPs) as the coating layer, for atrazine detection at ppb level on the basis of the direct competitive immunoassay procedures. Compared with the covalent-random antibody immobilization, the covalent-oriented strategy is more beneficial to improve the sensitivity of the nanobiosensor. Because the protein A is an interesting alternative to specifically bind with the Fc immunoglobulin region of the antibody, it was employed for oriented immobilization of the atrazine antibody [30], giving the highest immobilization density,

to exhibit better antigen binding efficiency and improve nanobiosensor's performance [31]. The direct competitive immunoassay for atrazine was constructed by oriented immobilization of atrazine antibody to protein A covalently modified on the AuNPs-coated ME material surface, followed by the competitive reaction of atrazine–albumin conjugate (Atr–BSA) and atrazine with the atrazine antibody. Atr–BSA was induced to amplify the signal responses, in turn significantly increasing the sensitivity of the nanobiosensor. The efficiency of the ME nanobiosensor was evaluated, demonstrating that a novel ME nanobiosensor for the detection of trace concentrations of atrazine was successfully developed.

## Materials and Methods

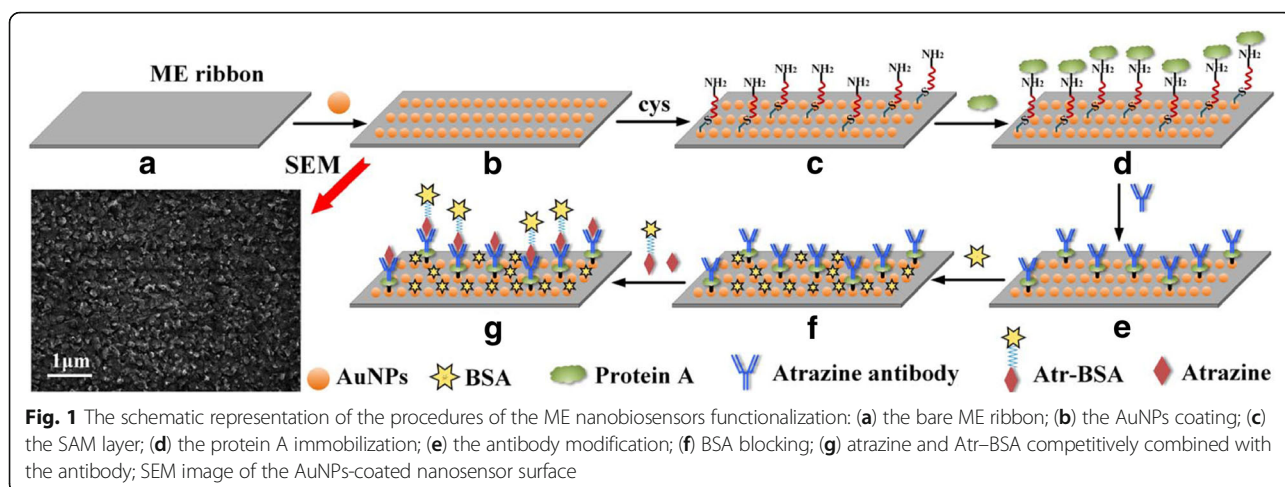
### Materials

Atrazine antibody, atrazine–albumin conjugate antigen (Atr–BSA), atrazine, and protein A were purchased from EastCoast Bio (Maine, USA). Simazine, prometryn, and dichlorodiphenyltrichloroethane (DDT) were obtained from Chengdu Huaxia Chemical Reagent Co., Ltd. Cysteamine, 1-ethyl-3-(3-dimethylaminopropyl) carbodiimide hydrochloride (EDC), *N*-hydroxysulfosuccinimide (NHS), bovine serum albumin (BSA, 99%), and phosphate-buffered saline (PBS buffer, pH = 7.4) were purchased from Sigma-Aldrich Corporation (Saint Louis, MO, USA).

### ME Nanobiosensor Fabrication

#### Preparation of the ME Nanosensor Platform

ME material ribbons composed of Metglas alloy 2826 ( $\text{Fe}_{40}\text{Ni}_{38}\text{Mo}_4\text{B}_{18}$ ) were purchased from Honeywell Corporation (Morristown, NJ, USA) and cut into 5 mm × 1 mm × 0.028 mm using a computer-controlled laser cutting machine. To remove organic film and debris, the ME ribbons were ultrasonically cleaned in acetone and ethanol each for 10 min and rinsed in deionized water, then dried in a stream of nitrogen (Fig. 1a). A ~100-nm-thick layer of chromium nanoparticles was sputtered on both sides of the ME ribbon surface to enhance the adhesion between the AuNPs and the ribbon surface. Subsequently, both sides of the chromium-coated ME ribbon surface were sputtered with AuNPs to improve the biocompatibility and protect the ribbon from oxidation and corrosion. The scanning electron microscope (SEM) image in Fig. 1 showed that the AuNPs coated on the ME ribbon were in spherical size. AuNPs and -SH can easily form the Au-S bond. Besides due to its attractive advantages of low-price, non-corrosion, biocompatibility, and nontoxicity [32], AuNPs can provide an excellent interface for the chemical or bio-recognition elements modification [33, 34]. Afterwards, the ME ribbons were annealed in a vacuum oven at 200 °C for 2 h to relieve residual



internal stress and promote the adhesion of the AuNPs layer to the ME ribbons. Then, the ME nanosensor platforms were finished and ready for atrazine antibody immobilization (Fig. 1b).

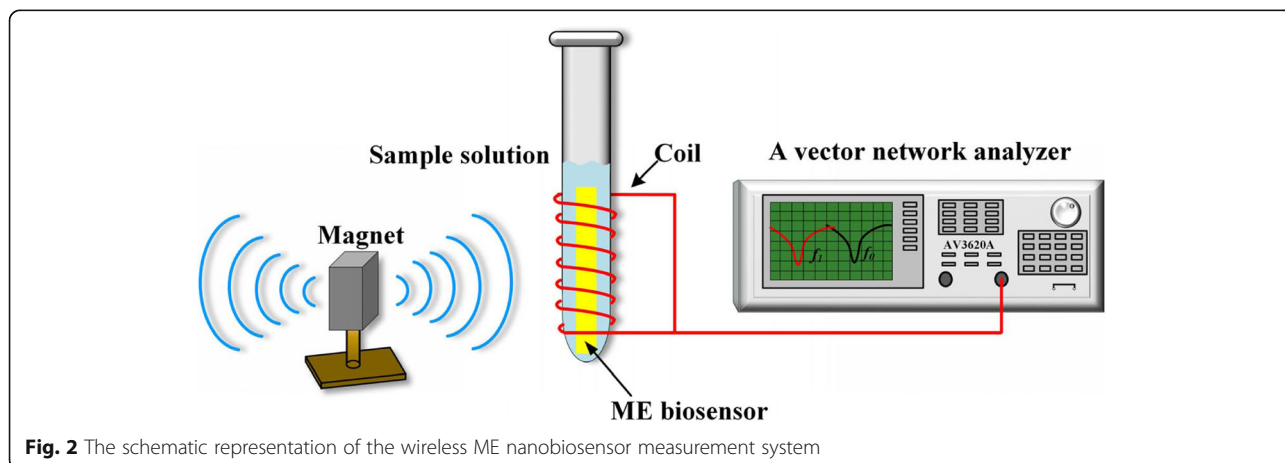
#### Atrazine Antibody Immobilization

The AuNPs-coated nanosensor platforms were ultrasonically cleaned with acetone, isopropanol, deionized water, and ethanol each for 5 min, and dried under a stream of nitrogen. Then, the nanosensor platforms were immersed into cysteamine solution (10 mM) for 12 h at room temperature to obtain a self-assembled monolayer (SAM) (Fig. 1c). The protein A (1 mg/mL) was activated with 4 mg/mL EDC-4 mg/mL NHS for 30 min at room temperature. After that, the activated protein A was incubated on the SAM-modified nanosensors for 30 min at 37 °C and rinsed with PBS buffer (Fig. 1d). The nanosensor platforms were then incubated with atrazine antibody for 50 min and washed with PBS buffer (Fig. 1e). To prevent non-specific adsorption, the atrazine antibody-coated nanosensors were further treated with

0.5% BSA for 30 min, and then rinsed with PBS buffer to remove any unbound BSA and dried under a nitrogen stream. Finally, the ME nanobiosensors were fabricated for atrazine detection (Fig. 1f).

#### Signal Measurement

The resonance frequency of the ME nanobiosensor was measured using a pickup coil wound around a vial, together with a vector network analyzer (AV3620A, the 41st Institute of CETC, Qingdao, China), as schematically represented in Fig. 2. To generate an alternating magnetic field, the network analyzer connected with the pickup coil was operated in the  $S_{11}$  mode for providing a swept frequency signal to the coil, and it can monitor the reflected signal from the coil. Additionally, a static magnetic field generated by a bar magnet was applied to enhance the resonance behavior. The nanobiosensors were vertically and wirelessly (without any wire connections with measurement system) inserted into the vial containing 30  $\mu$ L sample solutions to be tested. All experiments were conducted at room temperature ( $25 \pm 2$  °C) in



PBS (0.1 M, pH 7.4) solvent system. The resonance frequency of the nanobiosensor can be determined through the measurement of the  $S_{11}$  parameter, which was monitored and recorded every 5 min.

## Results and Discussion

### Characterization of the Nanobiosensor Surface

#### Morphology

Atomic force microscope (AFM, ND-100, Park System, Korea) observation of the nanobiosensor surface was performed to examine the immobilization effect of atrazine antibody. AFM images of the AuNPs-coated nanobiosensor and antibody-modified nanobiosensor surface are presented in Fig. 3a, b, respectively. It is clear that the increased surface roughness results from the covalently immobilized atrazine antibody. Comprehensive analysis of the AFM cross-sections topography shows that the AuNPs-coated nanobiosensor has the height variation of 13.421 nm; however, the value increased to 28.425 nm after the antibody modification. As well known that the diameter of the antibody molecular is about 15 nm, it is obviously concluded that the immobilization of atrazine antibody is successful.

#### Optimization for Concentration of Atrazine Antibody

The immobilization concentration of the antibody has an important influence on the sensitivity of the nanobiosensor. Therefore, it was necessary to evaluate the resonance frequency response of the nanobiosensor with different immobilization concentrations of atrazine antibody (25  $\mu\text{g/mL}$ , 50  $\mu\text{g/mL}$ , 75  $\mu\text{g/mL}$ , 100  $\mu\text{g/mL}$ ). From Fig. 4, we can see that the resonance frequency shift reached maximum at 50  $\mu\text{g/mL}$ . When the concentration of atrazine antibody went up to 75  $\mu\text{g/mL}$ , the response began to decline due to the steric hindrance and the electrostatic repulsion [35]. That is to say, the 50  $\mu\text{g/mL}$  atrazine antibody can attain relatively saturated immobilization. Thus,

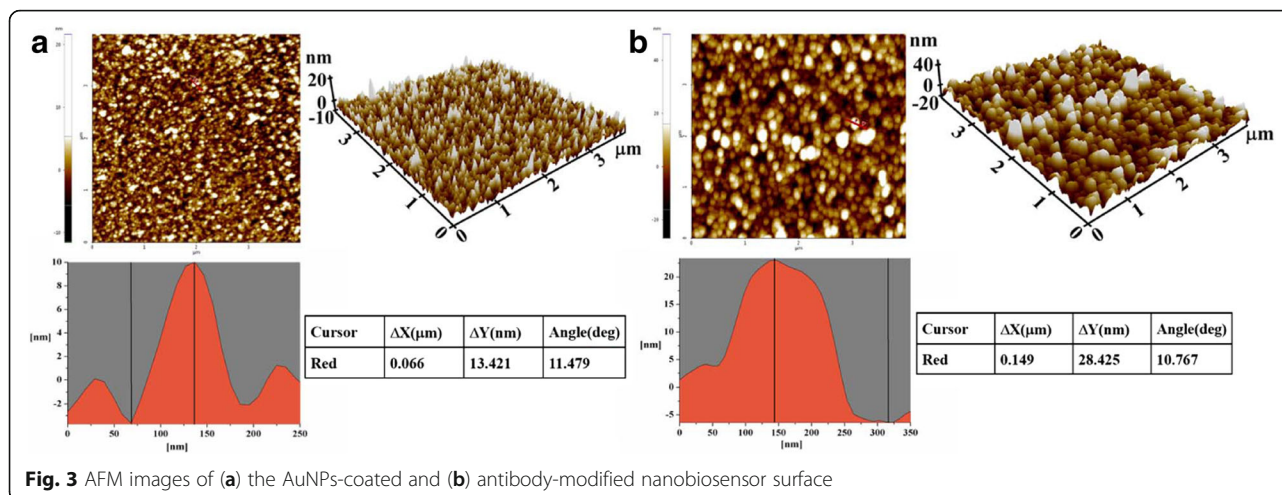
50  $\mu\text{g/mL}$  was the optimum concentration of atrazine antibody for immobilization.

#### Optimization for Concentration of Atr-BSA

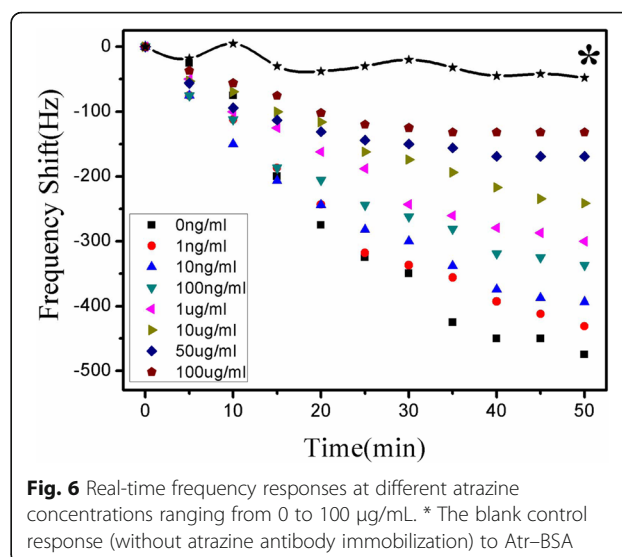
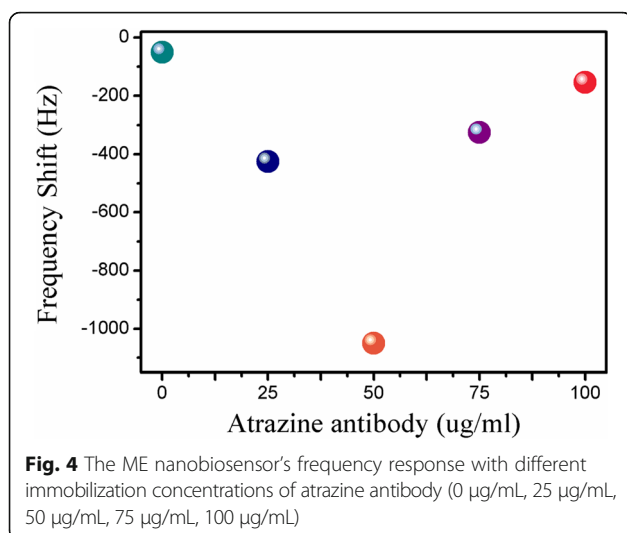
In the immunoreaction, atrazine and Atr-BSA competed for the limited number of atrazine antibody sites on the nanobiosensor surface. Hence, with the optimum concentration of atrazine antibody for immobilization, the working concentration of Atr-BSA, as an important factor, affects the sensitivity of the nanobiosensor. The optimization process was investigated by determining the ME nanobiosensor's resonance frequency response to Atr-BSA of different concentrations (20  $\mu\text{g/mL}$ , 40  $\mu\text{g/mL}$ , 60  $\mu\text{g/mL}$ , 80  $\mu\text{g/mL}$ ). As indicated in Fig. 5, the maximum response was observed at 40  $\mu\text{g/mL}$ . So 40  $\mu\text{g/mL}$  Atr-BSA was used in the following determination.

#### Atrazine Detection

Figure 6 depicts the real-time frequency response of the ME nanobiosensor measured in the sample mixture of 15  $\mu\text{L}$  Atr-BSA (40  $\mu\text{g/mL}$ ) and 15  $\mu\text{L}$  atrazine with different concentrations (0 ng/mL, 1 ng/mL, 10 ng/mL, 100 ng/mL, 1000 ng/mL, 10  $\mu\text{g/mL}$ , 50  $\mu\text{g/mL}$ , 100  $\mu\text{g/mL}$ ). As shown in Fig. 1g, atrazine and Atr-BSA competitively combined with the antibody immobilized on the nanobiosensor surface, which in turn leads to an increase of the mass load on the nanobiosensor surface, consequently causing a decrease of the resonance frequency with the incubation time. It is clear from Fig. 6 that the steady-state response is generally achieved at about 50 min. Atr-BSA concentration and the number of atrazine antibody sites were fixed, so the amount of bonded Atr-BSA on the nanobiosensor were inversely proportional to the concentration of atrazine in solution. The molecular weight of Atr-BSA is greater than that of atrazine. Therefore, the resonance frequency of the nanobiosensor changes inversely with the concentration





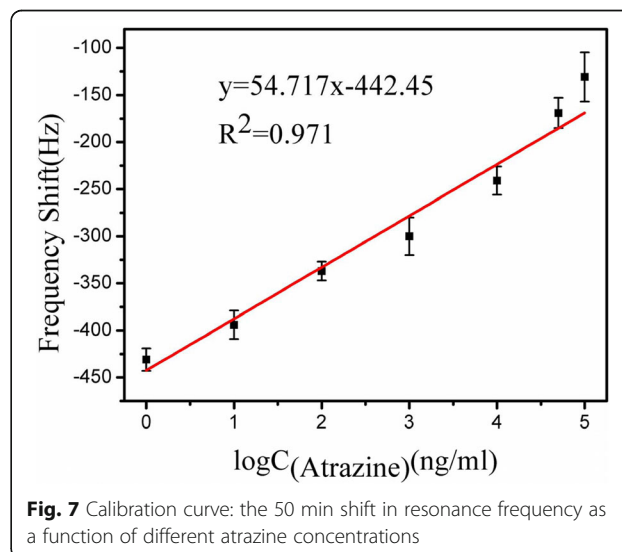
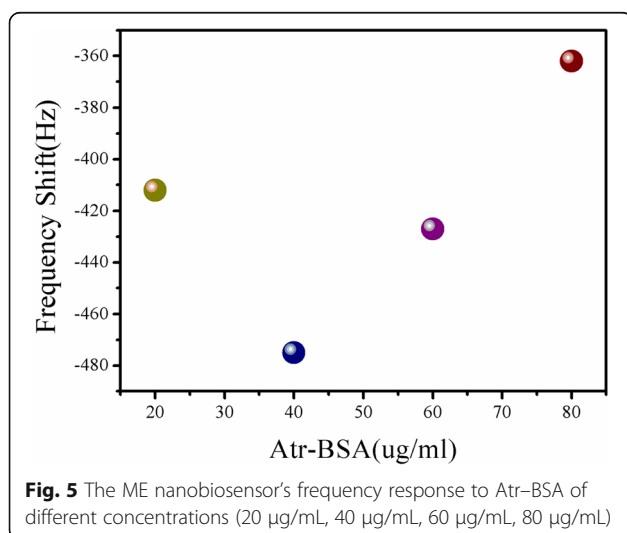


of atrazine in solution. As shown in Fig. 6, the rate and magnitude of the resonance frequency shift decreased with increasing atrazine concentrations, and a higher concentration of atrazine can induce a smaller resonance frequency shift. Figure 6 curve \* represents a background response of the blank control sensor (without atrazine antibody immobilization) to Atr-BSA, which is approximately 48 Hz far less than the detection signal, indicating that the non-specific adsorption can be ignored. Thus, the atrazine concentration can be detected through the resonance frequency shift of the wireless ME nanobiosensor, with an inversely proportional relation.

The standard calibration curve for the detection of atrazine on the ME nanobiosensor during the first 50 min are shown in Fig. 7. For each concentration, the nanobiosensor calibration experiments were conducted five times under identical conditions. It is found that the resonance frequency shift is linear with the logarithm value of the atrazine concentrations

ranging from 1 ng/mL to 100  $\mu\text{g/mL}$ , which can be represented by  $\Delta f = 54.717 \log C_{\text{Atrazine}} - 442.45$  ( $R^2 = 0.971$ ). The sensitivity is calculated to be  $3.43 \text{ Hz}/\mu\text{g mL}^{-1}$ . It is evident from Fig. 7 that the limit of detection (LOD) is 1 ng/mL, which is significantly lower than the upper permissible limit for atrazine of 3  $\mu\text{g/L}$  given in the US EPA, satisfying the standard currently available. Besides, the detection limit is evidently lower than that of the previous reported methods [36, 37]. It has been demonstrated that a low-cost, wireless, and highly sensitive nanobiosensor was successfully established for real-time detection of atrazine.

Since atrazine is the small molecule, direct competitive immunoassay approach was employed to improve the sensitivity of the ME nanobiosensor. In the direct competitive immunoassay, the antibody is modified on the



sensor surface and the signal response results from the binding of Atr-BSA molecule. Conversely, in the indirect competitive immunoassay, Atr-BSA is immobilized on the sensor surface and the response results from the binding of antibody molecule. According to the literature researches [38] and our results, the direct competitive immunoassay is feasible for small molecules monitoring. The indirect competitive immunoassay is highly sensitive to the analyte sample with trace concentration [39]. Although the indirect competitive immunoassay has a higher sensitivity [40, 41], it may be complicated to operate and difficult to implement for repeated reliable use [36]. However, the direct competitive immunoassay is very fast, simple to use, and self-contained—no additional reagents needed [36]. Thus, for the future development, the direct competitive immunoassay may be the most promising method.

### ME Nanobiosensor Specificity

The ME nanobiosensor specificity to atrazine was investigated by determining the nanobiosensor's responses to some other pesticides, such as prometryn, simazine, and DDT, as shown in Fig. 8. It was evident from Fig. 8 that the ME nanobiosensor showed little responses to these interferences due to non-specific absorption, and the responses to prometryn and simazine were slightly larger than DDT, which had a similar response level to the blank solution. It may be due to the fact that both prometryn and simazine have the similar structures with atrazine, belonging to triazine pesticides; however, DDT is a kind of organochlorine insecticides. The results indicated that atrazine was effectively recognized and specifically combined with the antibody immobilized on the nanobiosensor surface. Thus, the ME nanobiosensor showed strong specificity for atrazine detection.

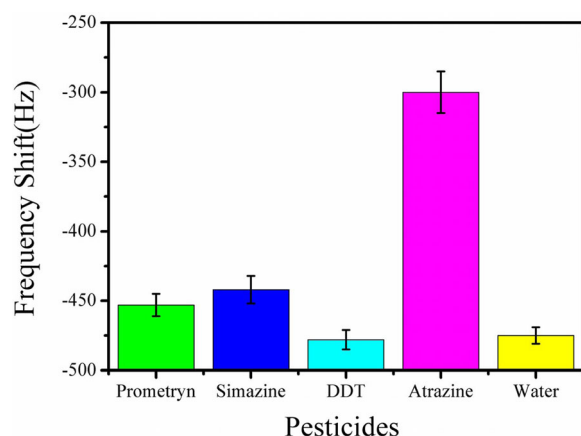


**Fig. 8** Resonance frequency response of the ME nanobiosensor to other interferences with the concentration of 100 µg/mL

### ME Nanobiosensor Stability

Figure 9 shows the stability of the ME nanobiosensor toward atrazine detection. Six of the same ME nanobiosensors were prepared and stored in 4 °C, every which was tested towards 10 ng/mL atrazine every other day until 6 days. Every single detection cycle only tested one nanobiosensor for 50 min. It is clear that the resonance frequency responses of the nanobiosensors remain nearly constant and the relative standard deviation (RSD) is calculated to be 1.8%. The result demonstrates that the ME nanobiosensor exhibits excellent stability for atrazine detection.

### Conclusions

A wireless ME nanobiosensor based on ME materials and AuNPs was successfully developed for real-time and highly sensitive detection of atrazine employing the competitive immunoassay. The oriented immobilization of atrazine antibody through protein A improved the nanobiosensor's performance. Atr-BSA with heavy molecule mass and atrazine competitively combined with atrazine antibody on the nanobiosensor surface, amplifying the signal responses, which in turn improved the sensitivity. The resonance frequency shift mainly induced by the bound Atr-BSA is inversely proportional to the target atrazine concentration. Besides, the working concentrations of atrazine antibody and Atr-BSA were optimized to be 50 µg/mL and 40 µg/mL, respectively. Under the optimum conditions, the ME nanobiosensor displays widely linear determination ranges for atrazine from 1 ng/mL to 100 µg/mL, with the satisfactory sensitivity of 3.43 Hz/µg mL<sup>-1</sup> and the detection limit of 1 ng/mL which is sufficient for the legislative requirements and is lower than other reported methods. AFM images verified that the atrazine antibody was successfully immobilized on the nanobiosensor surface in

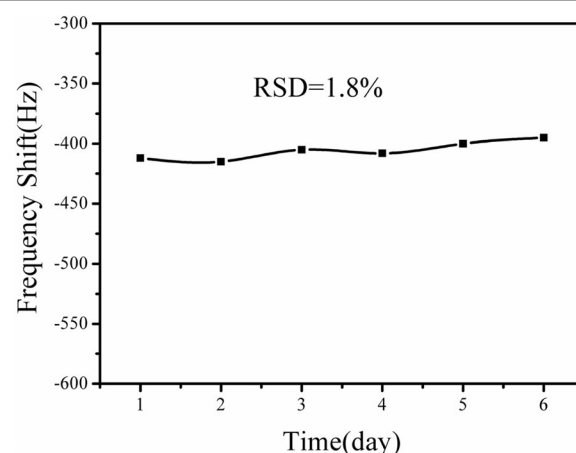


**Fig. 9** Stability measurements of 10 ng/mL atrazine on the ME nanobiosensor

an oriented manner. The experimental results demonstrate that the ME nanobiosensor has high specificity and stability toward atrazine. Benefiting from its effects on detection limits, simplicity, disposable property, and wireless nature, the study not only proposed a new method for highly sensitive detection of atrazine but also indicated its potential practicability for other environmental contaminants detection and water quality monitoring.

#### Abbreviations

AFM: Atom force microscope; Atr-BSA: Atrazine-albumin conjugate antigen; AuNPs: Gold nanoparticles; BSA: Bovine serum albumin; DDT: Dichlorodiphenyltrichloroethane; EDC: 1-Ethyl-3-(3-dimethylaminopropyl) carbodiimide hydrochloride; ME: Magnetoelastic; NHS: *N*-Hydroxysulfosuccinimide; PBS: Phosphate-buffered saline; SAM: Self-assembled monolayer; SEM: Scanning electron microscope; US EPA: Environmental Protection Agency in the United States

#### Acknowledgements

Not applicable.

#### Funding

The authors are grateful for the financial support from the National Natural Science Foundation of China (No. 51622507, 61471255, 61474079, 61501316, 51505324), Excellent Talents Technology Innovation Program of Shanxi Province of China (201605D211023).

#### Availability of Data and Materials

All data generated or analyzed during this study are included in this published article.

#### Authors' Contributions

SS and YZ designed the experiments; XG, RL, and JW performed the experiments; XG and JG analyzed the data; XG wrote the paper; and ZY and WZ discussed the results and commented on the manuscript. All authors read and approved the final manuscript.

#### Competing Interests

The authors declare that they have no competing interests.

#### Publisher's Note

Springer Nature remains neutral with regard to jurisdictional claims in published maps and institutional affiliations.

#### Author details

<sup>1</sup>MicroNano System Research Center, Key Lab of Advanced Transducers and Intelligent Control System of the Ministry of Education & College of Information Engineering, Taiyuan University of Technology, Jinzhong 030600, China. <sup>2</sup>Department of Biomedical Engineering, Shanxi Key Laboratory of Material Strength & Structural Impact, College of Mechanics, Taiyuan University of Technology, Jinzhong 030600, China.

Received: 16 November 2018 Accepted: 17 December 2018

Published online: 24 December 2018

#### References

- Huang X, Hou X, Zhang X, Rosso K, Zhang L (2018) Facet-dependent contaminant removal properties of hematite nanocrystals and their environmental implications. *Environ Sci Nano*
- Chen X, Pu H, Fu Z, Sui X, Chang J, Chen J, Mao S (2018) Real-time and selective detection of nitrates in water using graphene-based field-effect transistor sensors. *Environ Sci Nano*
- Li Z, Jiang Y, Liu C, Wang Z, Cao Z, Yuan Y, Li M, Wang Y, Fang D, Guo Z (2018) Emerging investigator series: dispersed transition metal on nitrogen doped carbon nanoframework for environmental hydrogen peroxide detection. *Environ Sci Nano*
- Arias-Estévez M, López-Periago E, Martínez-Carballo E, Simal-Gándara J, Mejuto J-C, García-Río L (2008) The mobility and degradation of pesticides in soils and the pollution of groundwater resources. *Agric Ecosyst Environ* 123:247–260
- González-Rodríguez R, Rial-Otero R, Cancho-Grande B, Gonzalez-Barreiro C, Simal-Gándara J (2011) A review on the fate of pesticides during the processes within the food-production chain. *Crit Rev Food Sci Nutr* 51:99–114
- Dagnac T, Bristeau S, Jeannot R, Mouvet C, Baran N (2005) Determination of chloroacetanilides, triazines and phenylureas and some of their metabolites in soils by pressurised liquid extraction, GC–MS/MS, LC–MS and LC–MS/MS. *J Chromatogr A* 1067:225–233
- Ali I, Allothman Z, Al-Warthan A (2016) Sorption, kinetics and thermodynamics studies of atrazine herbicide removal from water using iron nano-composite material. *Int J Environ Sci Technol* 13:733–742
- Prasad K, Prathish K, Gladis JM, Naidu G, Rao TP (2007) Molecularly imprinted polymer (biomimetic) based potentiometric sensor for atrazine. *Sensors Actuators B Chem* 123:65–70
- Ackerman F (2007) The economics of atrazine. *Int J Occup Environ Health* 13:437–445
- Schirhagl R, Latif U, Dickert FL (2011) Atrazine detection based on antibody replicas. *J Mater Chem* 21:14594–14598
- Hyer KE, Hornberger GM, Herman JS (2001) Processes controlling the episodic streamwater transport of atrazine and other agrichemicals in an agricultural watershed. *J Hydrol* 254:47–66
- Pichetsurthorn P, Vattipalli K, Prasad S (2012) Nanoporous impedemetric biosensor for detection of trace atrazine from water samples. *Biosens Bioelectron* 32:155–162
- Koivunen ME, Dettmer K, Vermeulen R, Bakke B, Gee SJ, Hammock BD (2006) Improved methods for urinary atrazine mercapturate analysis—assessment of an enzyme-linked immunosorbent assay (ELISA) and a novel liquid chromatography–mass spectrometry (LC–MS) method utilizing online solid phase extraction (SPE). *Anal Chim Acta* 572(2):180–189
- Li YN, Wu HL, Qing XD, Li Q, Li SF, Fu HY (2010) Quantitative analysis of triazine herbicides in environmental samples by using high performance liquid chromatography and diode array detection combined with second-order calibration based on an alternating penalty trilinear decomposition algorithm. *Anal Chim Acta* 678(1):26–33
- Ma WT, Fu KK, Cai Z, Jiang GB (2003) Gas chromatography/mass spectrometry applied for the analysis of triazine herbicides in environmental waters. *Chemosphere* 52(9):1627–1632
- Yu Z, Zhao G, Liu M, Lei Y, Li M (2010) Fabrication of a novel atrazine biosensor and its subpart-per-trillion levels sensitive performance. *Environ Sci Technol* 44:7878–7883
- Kouzoudis D, Grimes CA (2000) Remote query fluid-flow velocity measurement using magnetoelastic sensors. *J Appl Phys* 87:6301–6303
- Gao X, Zhen R, Zhang Y, Grimes CA (2009) Detecting penicillin in milk with a wireless magnetoelastic biosensor. *Sens Lett* 7:6–10
- Petridis C, Dimitropoulos P, Hristoforou E (2006) A new magnetoelastic device for sensing applications. *Sensors Actuators A Phys* 129:131–137
- Grimes CA, Roy SC, Rani S, Cai Q (2011) Theory, instrumentation and applications of magnetoelastic resonance sensors: a review. *Sensors* 11: 2809–2844
- Zeng K, Grimes CA (2004) Threshold-crossing counting technique for damping factor determination of resonator sensors. *Rev Sci Instrum* 75: 5257–5261
- Baimpos T, Gora L, Nikolakis V, Kouzoudis D (2012) Selective detection of hazardous VOCs using zeolite/Metglas composite sensors. *Sensors Actuators A Phys* 186:21–31
- Schmidt S, Grimes CA (2001) Characterization of nano-dimensional thin-film elastic moduli using magnetoelastic sensors. *Sensors Actuators A Phys* 94:189–196
- Kouzoudis D, Grimes CA (2000) The frequency response of magnetoelastic sensors to stress and atmospheric pressure. *Smart Mater Struct* 9:885
- Jain KG, Schmidt S, Ong KG, Mungle C, Grimes CA (2000) Magnetoacoustic remote query temperature and humidity sensors. *Smart Mater Struct* 9:502
- Cai QY, Cammers-Goodwin A, Grimes CA (2000) A wireless, remote query magnetoelastic CO<sub>2</sub> sensor. *J Environ Monit* 2:556–560
- Ong KG, Leland JM, Zeng K, Barrett G, Zourob M, Grimes CA (2006) A rapid highly-sensitive endotoxin detection system. *Biosens Bioelectron* 21:2270–2274
- Huang S, Yang H, Lakshmanan R, Johnson M, Wan J, Chen IH, Winkle Iii H, Petrenko V, Barbaree J, Chin B (2009) Sequential detection of *Salmonella*

- typhimurium and *Bacillus anthracis* spores using magnetoelastic biosensors. *Biosens Bioelectron* 24:1730–1736
29. Lu Q, Lin H, Ge S, Luo S, Cai Q, Grimes CA (2009) Wireless, remote-query, and high sensitivity *Escherichia coli* O157: H7 biosensor based on the recognition action of concanavalin a. *Anal Chem* 81:5846–5850
  30. Trilling AK, Beekwilder J, Zuilhof H (2013) Antibody orientation on biosensor surfaces: a minireview. *Analyst* 138:1619–1627
  31. Cecchet F, Duwez AS, Gabriel S, Jérôme C, Jérôme R, Glinel K, Demoustier-Champagne S, Jonas AM, Nysten B (2007) Atomic force microscopy investigation of the morphology and the biological activity of protein-modified surfaces for bio-and immunosensors. *Anal Chem* 79:6488–6495
  32. Matsishin M, Rachkov A, Lopatynskiy A, Chegel V, Soldatkin A, El'Skaya A (2017) Selective amplification of SPR biosensor signal for recognition of *rpoB*, gene fragments by use of gold nanoparticles modified by thiolated DNA. *Nanoscale Res Lett* 12:252
  33. Wei H, Abtahi SMH, Vikesland PJ (2015) Plasmonic colorimetric and SERS sensors for environmental analysis. *Environ Sci Nano* 2:120–135
  34. Walcarius A, Minter SD, Wang J, Lin Y, Merkoçi A (2013) Nanomaterials for bio-functionalized electrodes: recent trends. *J Mater Chem B* 1:4878–4908
  35. Cao C, Kim JP, Kim BW, Chae H, Yoon HC, Yang SS, Sim SJ (2006) A strategy for sensitivity and specificity enhancements in prostate specific antigen- $\alpha$ 1-antichymotrypsin detection based on surface plasmon resonance. *Biosens Bioelectron* 21:2106–2113
  36. Přibyl J, Hepel M, Halamek J, Skladal P (2003) Development of piezoelectric immunosensors for competitive and direct determination of atrazine. *Sensors Actuators B Chem* 91:333–341
  37. Tk L, Oyama M, Ikebukuro K, Karube I (2000) Detection of atrazine based on the SPR determination of P450 mRNA levels in *Saccharomyces cerevisiae*. *Anal Chem* 72:2856–2860
  38. Weller MG, Zeck A, Eikenberg A, NAGATA S, UENO Y, NIESSNER R (2001) Development of a direct competitive microcystin immunoassay of broad specificity. *Anal Sci* 17(12):1445–1448
  39. Xiao-hong Z, Bao-dong S, Han-chang S, Lan-hua L, Hong-li G, Miao H (2014) An evanescent wave multi-channel immunosensor system for the highly sensitive detection of small analytes in water samples. *Sensors Actuators B Chem* 198:150–156
  40. Hao XJ, Zhou XH, Zhang Y, Liu LH, Long F, Song L, Shi HC (2014) Melamine detection in dairy products by using a reusable evanescent wave fiber-optic biosensor. *Sensors Actuators B Chem* 204:682–687
  41. Liu L, Shan D, Zhou X, Shi H, Song B, Falke F, Leinseb A, Heideman R (2018) TriPlex™ waveguide-based fluorescence biosensor for multichannel environmental contaminants detection. *Biosens Bioelectron* 106:117–121

**Submit your manuscript to a SpringerOpen<sup>®</sup> journal and benefit from:**

- Convenient online submission
- Rigorous peer review
- Open access: articles freely available online
- High visibility within the field
- Retaining the copyright to your article

---

Submit your next manuscript at ► [springeropen.com](https://www.springeropen.com)